Zeng Xiaomei (Orcid ID: 0000-0001-9101-1677)

Tolstogouzov Alexander (Orcid ID: 0000-0001-8642-2674)

Small Al cluster ion implantation into Si and 4H-SiC

Zeng Xiaomei[1], Pelenovich Vasiliy*[,1], Ieshkin Alexei[2], Danilov Andrey[2,3], Tolstogouzov Alexander [1,4,5], Zuo Wenbin[1], Ranjana Jha[6], Devi Neena[1], Fu Dejun*[,1], Xiao Xiangheng*[,1]

[1]Department of Physics and Key Laboratory of Artificial Micro- and Nano-structures of Ministry of Education, Hubei Nuclear Solid Physics Key Laboratory and Center for Ion Beam Application, School of Physics and Technology, Wuhan University, Wuhan, 430072, China

[2]Faculty of Physics, Lomonosov Moscow State University, Leninskie gory, 1, Moscow, 119991, Russia

[3]Institute of Solid State Physics, Russian Academy of Sciences, Chernogolovka, 142432, Russia

[4]Ryazan State Radio Engineering University, Gagarin Str. 59/1, Ryazan, 390005, Russian Federation and

[5]Centre for Physics and Technological Research (CeFITec), Dept. de Física da Faculdade de Ciências e Tecnologia (FCT), Universidade Nova de Lisboa, Caparica, 2829-516, Portugal

[6]Department of Physics, Netaji Subhas Institute of Technology, University of Delhi, Dwarka Sector-3, New Delhi 110078, India

Email: Xiangheng Xiao* - xxh@whu.edu.cn

Fu Dejun*- djfu@whu.edu.cn

Vasiliy Pelenovich* - pelenovich@mail.ru

This article has been accepted for publication and undergone full peer review but has not been through the copyediting, typesetting, pagination and proofreading process which may lead to differences between this version and the Version of Record. Please cite this article as doi: 10.1002/rcm.8489

* Corresponding author

Abstract

Rationale: Continuously downscaling integrated circuit devices require fabrication of shallower p-n junctions. Ion implantation approach at low energy is subjected to low beam current due to the Coulomb repulsion. To overcome this problem cluster ions can be used for implantation. In comparison with single ions, the cluster ions possess lower energy per atom and reduced Coulomb repulsion resulting in high equivalent current.

Methods: In this study to carry out low energy implantation into single crystalline silicon and 4H-SiC samples we employ Al_n^- (n = 1 – 5) clusters with energy in the range of 5–20 keV. The Al clusters are obtained by Cs sputtering of Al rod. Time-of-flight secondary ion mass spectrometry (IONTOF TOF.SIMS-5) is used to study aluminum and oxygen sputter depth profiles for different cluster sizes and implantation energies before and after annealing treatment.

Results: A distinguishable effect of the energy per atom in the cluster on reduction of the projected range R_p is revealed. The lowest R_p of 3±1 nm has been achieved in SiC samples at the energy per atom of 1.66 keV. After annealing of Si samples, a considerable change of the Al profiles due to redistribution of Al atoms during motion of the front of recrystallization is observed. The influence of the number of atoms in the cluster at the same energy per atom within the experimental uncertainty is not observed.

Conclusions: The transient effects of the sputtering by the primary ion beam distort the shape of the Al profiles in Si samples. In the case of SiC, due to its relatively lower surface

chemical activity, more informative ToF-SIMS depth profiling of the shallow cluster implantation is feasible.

Introduction

Recently, continuously smaller integrated circuit devices such as computers and mobile communication equipment have led to an ongoing need to fabricate shallow junctions, which have already broken through less than 7 nm ultra-shallow doping in silicon wafers [1]. Ion implantation would be difficult to be replaced in the manufacture of advanced semiconductor devices due to the concentration control, accuracy and stability of the injection depth, and repeatability. To meet the requirements of shallow junction depth, besides reducing ion energy and change of the incident angle, the implantation of polyatomic ions (clusters) has become a practical and feasible approach. Advantages of the cluster implantation are: (i) a $1/n$ partitioning factor for the implantation energy (where n is the number of atoms in the cluster), (ii) a $n^{5/2}$ amplification factor for the beam transport gain, due to reduction of the space charge effect [2, 3], (iii) a $1/n$ reduction factor for the implantation time with the same current [3], and (iv) a non-linear factor [4] for the implantation-induced damage, which suppresses transient-enhanced diffusion during annealing treatment [5].

In shallow implantation, most researchers choose an injection of B into Si, since B possesses the highest solid solubility with low acceptor ionization energy and hence high electrical activity. However, an effect of "channeling-tail" results in broadening of depth profiles. Young et al. implanting ^{11}B into silicon at 35 keV have showed that the depth profiles also have very evident "tail" after thermal and especially laser annealing [6]. Later it

has been shown that the "channeling-tail" effect can be reduced by implantation of SiB polyatomic ions instead of B single ions [7]. It was also found that if the energy decreased from 1 keV to 100 eV, the effect of reduction of projected range is cancelled out by transient enhanced diffusion during a rapid thermal annealing [8]. Takeuchi et al. have shown feasibility of using polyatomic molecular decaborane ($B_{10}H_{14}$), as a kind of B cluster to form shallow p^+/n junctions [5]. Recently, Krügener et al. have used ion implantation of amorphizing species of BF_x (x = 1, 2) to lower the thermal budget of annealing for formation of n-type silicon solar cells [9]. Aluminum is another p-type dopant of Si, which almost is not used due to its lower solubility at the level of 2×10^{19} cm^{-3} at 1100 ˚C in comparison with that of B, 4.5×10^{20} cm^{-3} at 1150 ˚C [10]. However, using the SRIM code it can be shown that Al ions of same energy have higher stopping power in comparison with B, which facilitates shallow implantation [11]. Al implantation with energy of 200 keV in Si (100) was studied by Sadana et al. [10]. Upon annealing Al was redistributed anomalously: the depth distribution had a few peaks, which were explained by the formation of defect layers due to the segregation of Al in precipitates, stimulated by its low solubility. An attempt to use low-energy shallow implantation of Al in Si was made by Hönicke et al. [12]. Al implanted in Si at energies in the range of 1 – 50 keV was studied by secondary ion mass spectrometry (SIMS) and synchrotron radiation-based depth-sensitive X-ray fluorescence techniques. The projected range less than 4 nm was reached at the energy of 1 keV. In another study carbon clusters such as C_3H_5 and C_2H_5 have been used for special shallow defect formation in silicon, such defects possessing high gettering capability for metal ions can improve CMOS image sensor parameters [13].

Nowadays, SiC is studied as a material for high-voltage and high temperature applications, due to its wide band gap, high thermal conductivity, and large breakdown electric field [14,15]. However, thermal diffusion doping requires temperatures more than 1700 ˚C because of very low diffusion coefficients of impurities [16]. Therefore, the ion implantation becomes an essential method of SiC doping. Al and B are mostly used as p-type dopants, and Al has an advantage of small redistribution after thermal annealing [17]. Recently, small clusters of C_6 were proposed to reduce graphitization temperature for graphene synthesis on 6H–SiC substrate [18].

To the best of our knowledge, presently there is lack of publications on solid-state cluster implantation into semiconductors, especially for SiC. In this work, we show advantages of the aluminum implantation, such as high stopping power, and the cluster effect (reduced energy per atom in the cluster) for further reduction of the implantation depth. We deploy small Al-clusters extracted from a source of negative ions by cesium sputtering (SNICS) to dope the single crystal n-Si and 4H-SiC. The Al target is a convenient material for SNICS, which can produce intense negative cluster ion beam.

Experimental details

Al_n^- (n = 1 – 5) cluster ions were produced by a SNICS source discussed elsewhere [19]. The Al target was prepared of a pressed Al powder (>99 % purity, Sinopharm Group Chemical Reagent Company). The cluster ion current is ranged from 1.5 μA (n = 2) to 0.27 μA (n = 5) at the accelerating voltage of 20 kV. The cluster ions with a desired number of atoms are selected by the electromagnet with the magnetic field up to 0.7 T.

The samples were single crystal n-Si (10×10 mm^2 in size, thickness of 0.5 mm, <100> orientation, resistivity of 10 Ω·cm, doped with P, oxygen content <18 ppm) and 4H-SiC plates (10×10 mm^2 in size, thickness of 0.3 mm, <0001> orientation, Si-faced, Hefei Kejing Material Tech. Co. Ltd.). Before the ion implantation, the Si samples were rinsed in 5% HF solution to remove the surface oxide layers. Al_n^- (n = 1 – 5) cluster were used as projectiles. The cluster ion implantation was performed at the dosage of 10^{15} atoms/cm^2 and energy in the range of 5 – 20 keV through a 5×5 mm^2 aperture near the irradiated sample at room temperature. The dose is defined as the number of atoms (but not clusters) per square cm. To improve the homogeneity of the implanted aluminum we used defocusing of the ion beam, which results in decrease of the beam current in ~10 times. To suppress the channeling effect during implantation the surface normal of the samples was tilted to 10 degree relative to the cluster beam. After implantation, the samples were annealed at 800 ℃ for 30 min in Ar atmosphere (P_{Ar} = 1 atm) to recover the crystal structure.

SRIM-2013 code was used to simulate implantation depth profiles. As a binary collision model, SRIM-2013 is not directly applicable for the cluster ion implantation, which is known to be complicated by the "clearing-the-way" effect resulting in increased projected range [20]. Therefore, SRIM-2013 can be used only as a first approximation. In simulation we use the same tilt of 10 degree and appropriate energy per atom *E/n*, where *E* is the cluster ion energy and *n* is the number of atoms in the cluster, 100000 Al projectiles were used.

Fig. 1a shows mass-spectrum of the negative cluster ions obtained from the Al target. Besides Al clusters, atomic oxygen and AlO^- ions originating from the naturally oxidized surface layer of the Al particles are observed. An advantage to use cluster ions instead of

single ions is demonstrated in Fig. 1b. The equivalent current calculated as a product of measured current and the number of atoms in the cluster is shown as a function of the energy per atom calculated as a ratio of the cluster energy and number of atoms in the cluster. All clusters demonstrate equivalent current, which is more than one order of magnitude higher than the single ion current at the same energy per atom. At the accelerating voltage less than 5 kV the beam current decreases sharply, therefore, only cluster ions can be used at the energy per atom lower than 5 keV.

The prepared samples were characterized by means of the time-of-flight secondary ion mass spectrometry (ToF-SIMS) using an IONTOF TOF.SIMS-5 apparatus at ISSP RAS (Moscow, Russian Federation).The instrument operated in the dual beam mode employing 1 keV/80 nA Cs^+ or 1 keV/150 nA O_2^+ sputtering beams scanned over an area of 250 × 250 μm^2 and pulsed 25 keV/1 pA Bi^+ ion beam for analysis scanned over an area of 50 × 50 μm^2 in the center of the sputtered zone. Both beams were incident at 45° from the normal. Elemental in-depth profiles were measured in 2-3 different points of the sample surface for each cluster species and implantation energy.

The implantation depth was estimated by the crater depth measurement using an AMBIOS XP-1 stylus-type profilometer under assumption of a constant sputter rate. The experimental uncertainty of the sputter rate and, correspondingly, the projected range R_p, is estimated at 5%. These parameters (R_p and longitudinal range straggling ΔR_p) were calculated using fitting by the Pearson IV distribution. It should be noted that the contribution of the analysis ion beam in the total sputter rate is negligible since under our experimental conditions the sputter rate ratio is higher than 250. It means that the analysis beam erodes less

than 0.4 % of the sample material being sputtered. Presently, the value of the sputter rate ratio in the range of a few hundred up to thousand is typical for the most part of depth profiling using modern ToF-SIMS instrumentation [21]. Intensities of Al signal in depth profiles were recalculated into bulk concentration using the value of relative sensitivity factor (RSF) for Al in Si [22] and Al in SiC [23].

Results and discussion

Fig. 2a shows ToF-SIMS aluminum depth profiles after Al_n (n = 1, 2, 3, and 5) cluster implantation into n-Si at 10 keV and dose of 10^{15} atoms/cm^2 before annealing as well as TRIM simulated profiles of aluminum ions at corresponding energy per atom [11]. Fig. 2b shows profiles after Al_n (n = 2, 3, and 5) cluster implantation at 20 keV and corresponding simulations. The simulated profiles were normalized to the experimental profiles. The experimental and simulated projected ranges R_p and longitudinal straggling ΔR_p are shown in Table 1. As expected, the projected range decreases along with the energy per atom in the cluster. Comparison of the implantation of cluster Al_2 at 20 keV and atomic Al_1 at 10 keV, i.e. with the same energy per atom, shows similar projected range of ~16 nm. Therefore, within the experimental uncertainty one can conclude the absence of any visible nonlinear effects caused by an interaction between atoms of Al_2 cluster. All experimental ToF-SIMS profiles have wider descending shoulders. These deviations (“tails”) can be explained by not completely suppressed channeling effect [10] and knock-on and mixing effects of SIMS. The greatest deviation both of the projected range and profile shape from the simulated profiles is observed for the clusters with the lowest energy per atom. Such profile deviations at the

surface are explained by transient effects, which appear at the very beginning of the sputtering by the primary beam in SIMS. It corresponds to the depth, usually from 1 to 3 nm, to be sputtered before the erosion becomes stationary and a steady equilibrium between implanted and re-sputtered primary ions has been established [24]. However, even with this effect the decrease of the R_p along with decreasing energy per atom are clearly observed. The decrease of *Rp* is also proved by a shift of descending shoulders of the profiles towards the surface, which are less subjected to the transient effect.

Fig. 3a shows aluminum profiles after Al_n (n = 2 – 4) clusters implantation into 4H-SiC at 10 keV and dose of 10^{15} atoms/cm^2 before annealing and simulated by SRIM-2013 code profiles [11]. In Fig. 3b the profiles after Al_3 cluster implantation at energies of 5 – 20 keV and the same dose are presented. Similar to implantation into Si the projected range decreases along with the energy per atom in the cluster (see Table 2). The transient effect is also present, but to a much lesser extent compared with Si samples. This fact allows to observe clearly the implantation profile with the projected range of 3±1 nm for clusters with energy per atom only 1.66 keV. Another reason for the poorer lack of agreement between the experimental data and calculation for Si profiles can be the influence of a native oxide layer, which is absent in the case of SiC.

To recover Si crystal structure, furnace annealing at 800 ℃ for 30 min was performed. Fig. 4 shows Al profiles after implantation with Al_2 clusters at 20 keV and dose of 10^{15} cm^{-2} before and after annealing. After annealing the maximum of the Al distribution is shifted towards the surface; moreover, small additional peaks have appeared at 20 and 40 nm. Such change of the profile can be explained by the process of recrystallization of the surface

amorphous layer during annealing and the limited solubility of Al in the crystalline Si [10]. The recrystallization of the surface amorphous layer starts from the amorphous/crystalline interface, which is located at the deep edge of the profile. During annealing the interface is moved towards the surface. Since the solubility of Al in the crystalline Si is limited, the Al atoms are pushed ahead of the amorphous/crystalline interface. Therefore, most of Al atoms are transferred to the surface layer, where the recrystallization is finished. The small additional peaks appear due to the segregation of aluminum into precipitates. The formation of the peak at the depth of 40 nm is promoted by a defect layer (dislocations and vacancies) at the initial amorphous/crystalline interface [10,25], whereas, the peak at the depth of 20 nm can be originated by the defects in the region where the concentration of vacancies is maximal. In Fig. 4 the depth profiles of oxygen before and after annealing are also shown. The oxygen in the surface oxidized layer is observed as a peak in the range within 0-10 nm. The oxygen dissolved in the Si wafer is observed at a constant level of about 10^{18} cm^{-3}. After annealing procedure, the concentration of oxygen in the surface layer increases, probably due to small oxygen contamination of the argon atmosphere. The authors of Ref. [10] have found an apparent correlation for aluminum and oxygen profiles after an annealing procedure. It was considered a role of oxygen in pinning of the aluminum precipitates. However, in our experiment we have not observed any correlation in the profiles of these two elements. Therefore, it can be concluded that in the case of low energy cluster implantation there is no influence of bulk oxygen on the aluminum precipitate formation during the annealing process.

Conclusion

We have performed Al_n (n = 1 – 5) cluster implantation into n-type single crystalline Si and 4H-SiC. Aluminum clusters were produced by the SNICS source. The implantation energies of 10 or 20 keV and dose of 10^{15} atoms/cm^{-2} were used. The depth distribution of the aluminum measured by ToF-SIMS shows evident dependence of the projected range R_p on the energy per atom in the cluster. The R_p is changed from 16.1±0.7 to 3±2 nm in the energy per atom range 10 – 2 keV in Si substrate and from 9.2±0.6 to 3±1 nm in the energy per atom range 20 – 5 keV in SiC substrate. However, due to the transient effects as well as enhanced surface activity in the case of Si substrates ToF-SIMS depth profiles for low energy per atom implantation demonstrate shallower and distorted distributions in comparison with those simulated by TRIM. Any influence of the number of atoms in the cluster at the same energy per atom is not observed within the experimental uncertainty. To recover Si crystal structure after implantation we use furnace annealing at 800 ℃ for 30 min in an argon atmosphere. ToF-SIMS profiles of the post-annealed samples reveal considerable change of the Al distribution, which is explained by the process of the recrystallization of the surface amorphous layer during annealing and the limited solubility of Al in the crystalline Si. The process of redistribution of Al during the annealing results in the pushing of dopants towards the surface. Moreover, the annealing process results in Al precipitate formation, which is not related to the oxygen content of the bulk Si.

Acknowledgments

This work was supported by the National Natural Science Foundation of China under

grant 11875210, the International Cooperation Program of Guangdong Province Science and Technology Plan Project (2018A050506082), and China Postdoctoral Science Foundation under grant 2018M640724.

References

[1] Huang YC, Chiang MH, Wang SJ. Fossum JG. GAAFET Versus Pragmatic FinFET at the 5 nm Si-Based CMOS Technology Node. *IEEE J Electron Devi*. 2017;5:164-169.

[2] Moffatt S. Ion implantation from the past and into the future. *Nucl Instr Meth B*. 1995;96:1-6.

[3] Liang JH, Han HM, Range parameters of B_n cluster ion implantation in silicon. *Nucl Instr Meth B*. 2004;219–220:783-787.

[4] Aoki T, Matsuo J, Takaoka G, Toyoda N, Yamada I. Defect characteristics by boron cluster ion implantation. *Nucl Instr Meth B*. 2003;206:855-860.

[5] Takeuchi D, Shimada N, Matsuo J, Yamada I. Shallow junction formation by polyatomic cluster ion implantation. *Nucl Instr Meth B*. 1997;121:345-348.

[6] Young RT, White CW, Clark GJ, Narayan J, Christie WH, Murakami M, King PW, Kramer SD. Laser annealing of boron‐implanted silicon. *Appl Phys Lett*. 1978;32:139-141.

[7] Liang JH, Chiang SL, Chen CT. Depth profiles of cluster-ion-implanted BSi in silicon. *Nucl Instr Meth B*. 2002;190:767-771.

[8] Collart EJH, Weemers K, Gravesteijn DJ. Characterization of low-energy (100 eV–10 keV) boron ion implantation. *J Vac Sci Technol B*. 1998;16:280-284.

[9] Krügener J, Peibst R, Bugiel E, Tetzlaff D, Kiefer F, Jestremski M, Brendel R, Osten HJ.

Ion implantation of boric molecules for silicon solar cells. *Sol Energ Mater*. 2015;142:12-17.

[10] Sadana DK, Norcott MH, Wilson RG, Dahmen U. Transmission electron microscopy of aluminum implanted and annealed (100) Si: Direct evidence of aluminum precipitate formation. *Appl Phys Lett*. 1986;49:1169-1171.

[11] www.srim.org

[12] Hönicke P, Kayser Y, Beckhoff B, Müller M, Dousse JCl, Hoszowska J, Nowak SH. Characterization of ultra-shallow aluminum implants in silicon by grazing incidence and grazing emission X-ray fluorescence spectroscopy. *J Anal At Spectrom*. 2012;27:1432-1438.

[13] Okuyama R, Masada A, Shigematsu S, Kadono T, Hirose R, Koga Y, Okuda H, Kurita K. Effect of dose and size on defect engineering in carbon cluster implanted silicon wafers. *Jpn J Appl Phys*. 2018;57:011301.

[14] Casady JB, Johnson RW. Status of silicon carbide (SiC) as a wide-bandgap semiconductor for high-temperature applications: a review. *Solid-State Electronics*. 1996;39:1409-1422.

[15] Zhang Y, Sheng K, Su M, Zhao JH, Alexandrov P, Fursin L. 1000-V 9.1-m$\Omega\cdot$cm^2 Normally Off 4H-SiC Lateral RESURF JFET for Power Integrated Circuit Applications. *IEEE Electron Device Letters*. 2007;28:404-407.

[16] Properties of Silicon Carbide, ed. Harris GL, emis datareviews, Ser. No. 13, INSPEC, IEEE, London, U.K.

[17] Saks NS, Agarwal AK, Ryu SH, Palmour JW. Low-dose aluminum and boron implants in 4H and 6H silicon carbide. *J Appl Phys*. 2001;90:2796-2805.

[18] Zhang R, Li H, Zhang ZD, Wang ZS, Zhou SY, Wang Z, Li TC, Liu JR, Fu DJ.

Graphene synthesis on SiC: Reduced graphitization temperature by C-cluster and Ar-ion implantation. *Nucl Instr Meth B*. 2015;356-357:99-102.

[19] Wang ZS, Zhang ZD, Zhang R, Wang SX, Fu DJ, Liu JR. An ultralow-energy negative cluster ion beam system and its application in preparation of few-layer graphene. *Chin Sci Bull*. 2012;57:3556-3559.

[20] Popok VN, Barke I, Campbell EEB, Meiwes-Broer KH. Cluster–surface interaction: From soft landing to implantation. *Surf Sci Rep*. 2011;66:347-377.

[21] Grehl T, Möllers R, Niehuis E. Low energy dual beam depth profiling: influence of sputter and analysis beam parameters on profile performance using TOF-SIMS. *Appl Surf Sci*. 2003;203-204:277-280.

[22] Wilson RG. SIMS quantification in Si, GaAs, and diamond - an update. *Int J Mass Spectrom*. 1995;143:43-49.

[23] Kudriavtsev Yu, Villegas A, Godines A, Asomoza R, Usov I. Quantitative SIMS analysis of SiC. *Surf Interface Anal*. 2003;35:491–495.

[24] Hönicke P, Beckhoff B, Kolbe M, Giubertoni D, van den Berg J, Pepponi G. Depth profile characterization of ultra shallow junction implants. *Anal Bioanal Chem*. 2010;396:2825-2832.

[25] Sadana DK, Washburn J, Booker GR. Recrystallization of buried amorphous layers and associated electrical effects in P^+-implanted Si. *Philos Mag B*. 1982;46:611-633.

Table 1. Comparison of simulated and experimental profile parameters for implantation into Si.

Energy per atom, keV	Simulated R_p / ΔR_p for Al_1, nm	Experimental R_p / ΔR_p, nm			
		10 keV		20 keV	
10	20.8±0.3 / 12.4±1.3	Al_1	16.1±0.7 / 14.8±0.7	Al_2	15.5±0.8 / 14.2±0.6
6.66	15.1±0.2 / 8.7±0.7	-		Al_3	12.4±0.7 / 11.8±0.5
5	12.1±0.1 / 6.6±0.3	Al_2	9.9±0.8 / 6.1±0.5	Al_4	9.0±0.7 / 5.8±0.5
4	10.1±0.1 / 5.6±0.2	-		Al_5	4±2 / 3±1
3.33	8.9±0.1 / 4.9±0.1	Al_3	6±1.5 / 3±1	-	
2	6.2±0.1 / 3.4±0.1	Al_5	3±2 / 3±1		

Table 2. Comparison of the simulated and experimental profile parameters for implantation into 4H-SiC.

Energy per atom, keV	Simulated R_p / ΔR_p for Al_1, nm	Experimental R_p / ΔR_p, nm			
		10 keV		Al_3	
6.66	9.7±0.1 / 4.5±0.2	-		20 kV	9.2±0.6 / 5.5±0.4
5	7.8±0.1 / 3.7±0.1	Al_2	7.1±0.5 / 4.4±0.3	15 kV	6.5±0.4 / 4.5±0.3
3.33	5.8±0.1 / 2.8±0.1	Al_3	5.0±0.5 / 3.4±0.3	10 kV	5.0±0.5 / 3.4±0.3
2.5	4.7±0.1 / 2.3±0.1	Al_4	3.5±0.7 / 3.1±0.3	-	
1.66	3.5±0.05 / 1.7±0.1	-		5 kV	3±1 / 1.4±0.3

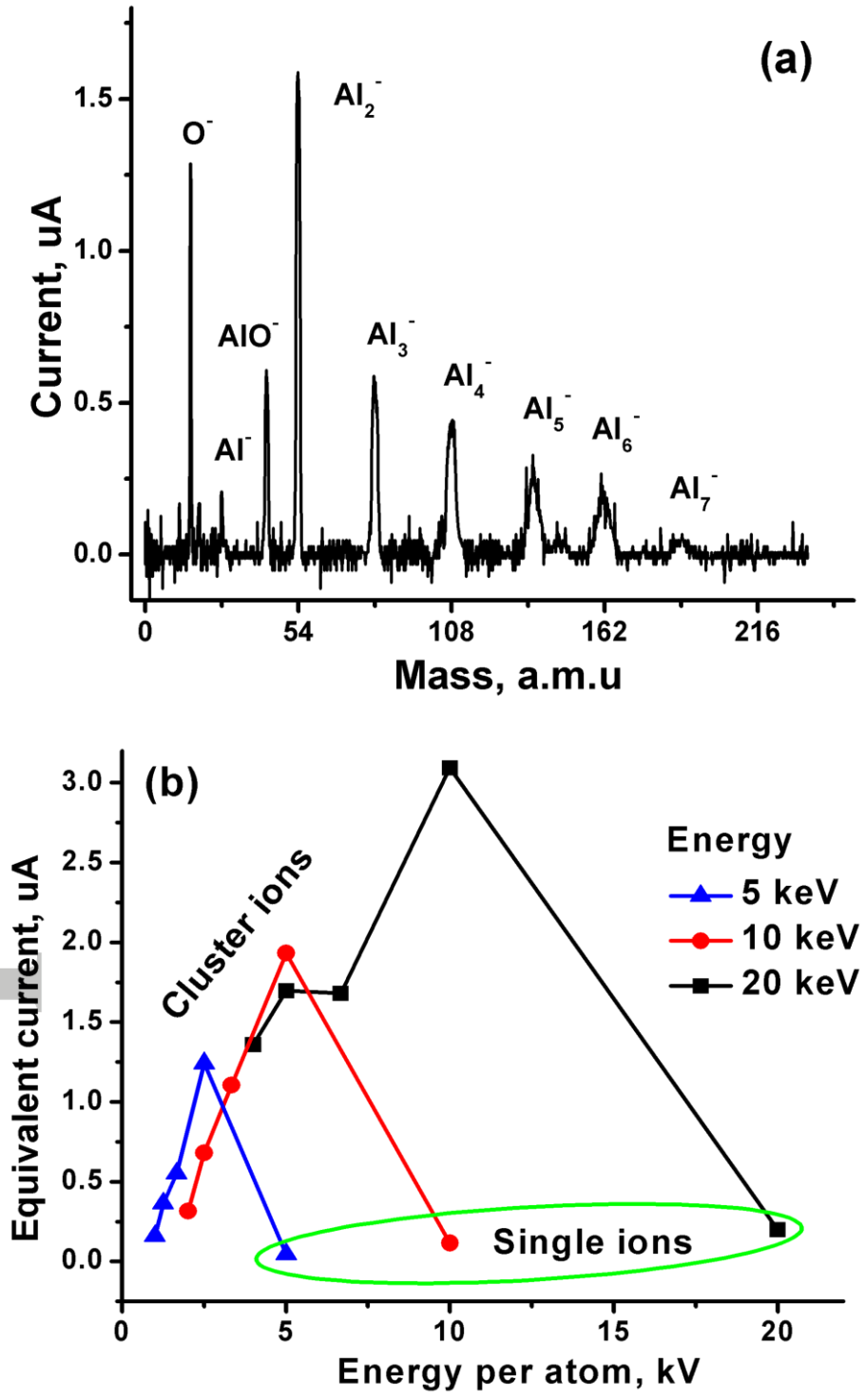

Fig. 1. Mass spectrum of the cluster ion beam at 20 keV formed by Al target (a). Equivalent currents of Al_n (n = 1 – 5) cluster ions at different energy (b).

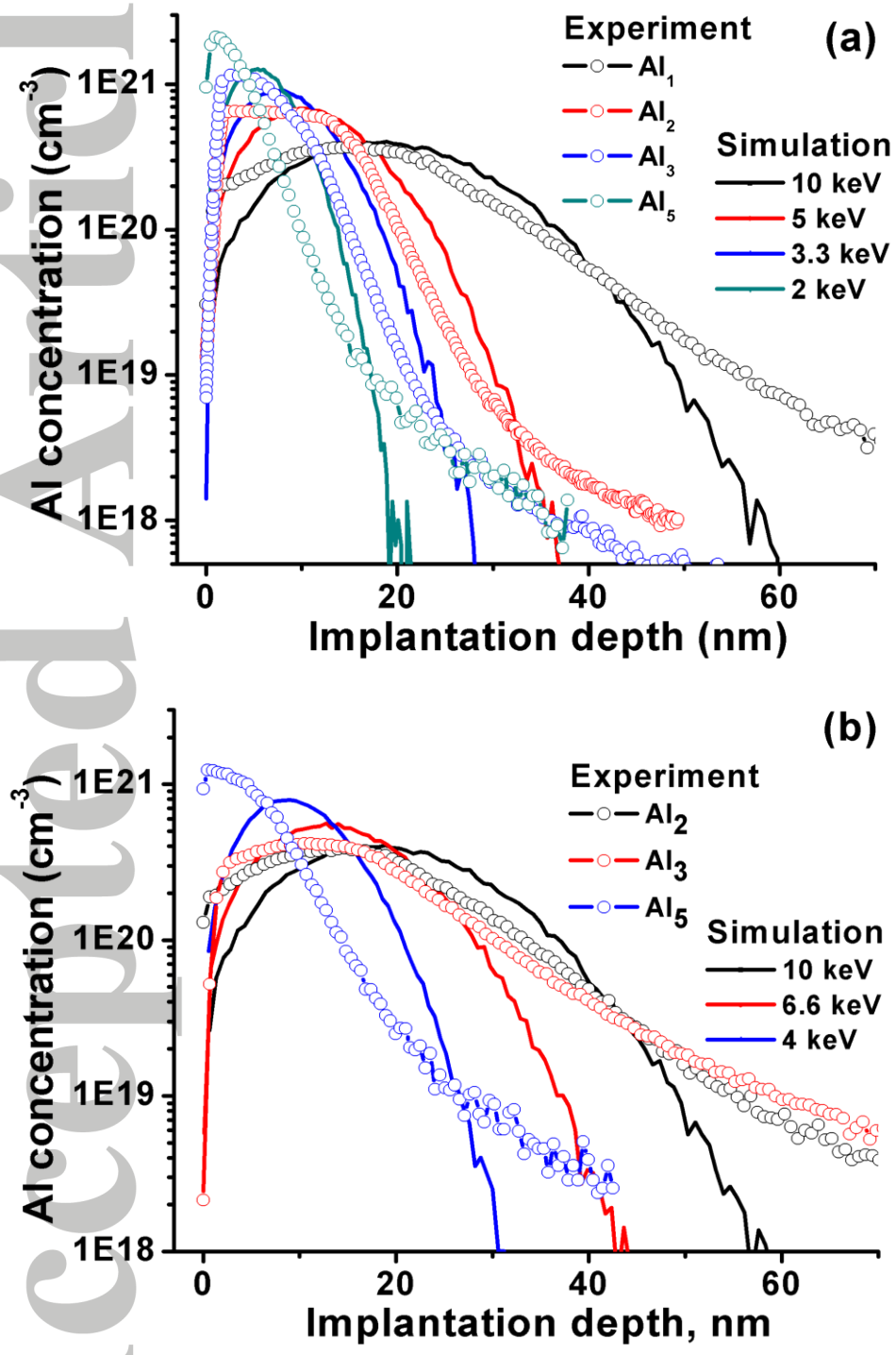

Fig.2. ToF-SIMS depth profiles of aluminum implanted into n-Si at dose of 10^{15} atoms/cm^2 before annealing and simulated profiles with corresponding energy per atom: Al_n (n = 1, 2, 3, and 5) clusters implanted at 10 keV (a) and Al_n (n = 2 , 3, and 5) clusters implanted at 20 keV

(b).

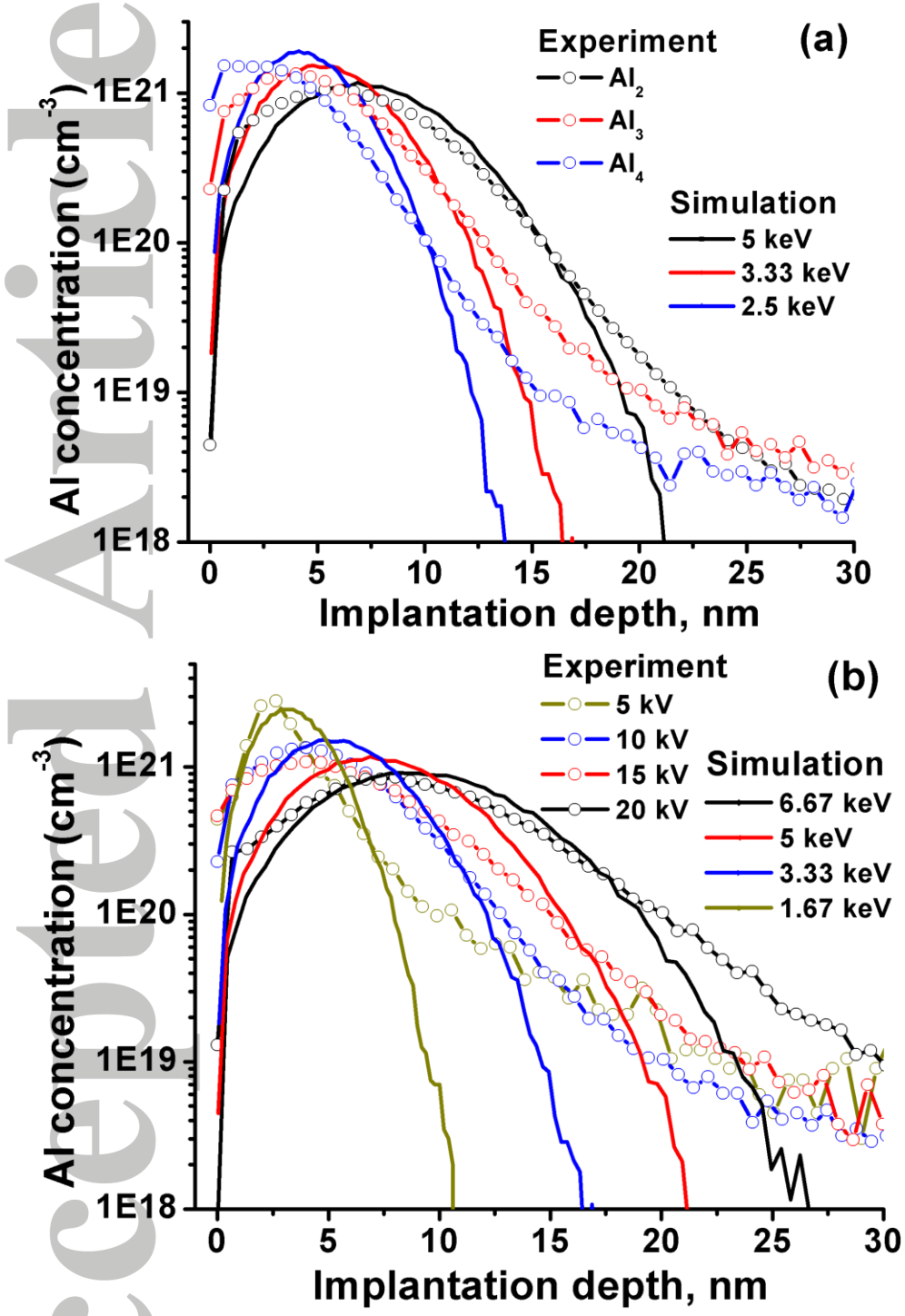

Fig.3. ToF-SIMS depth profiles of aluminum implanted into 4H-SiC and simulated profiles with corresponding energy per atom: Al_n (n = 2 – 4) clusters implanted at 10 keV (a) and Al_3 clusters implanted at 5, 10, 15, and 20 keV (b).

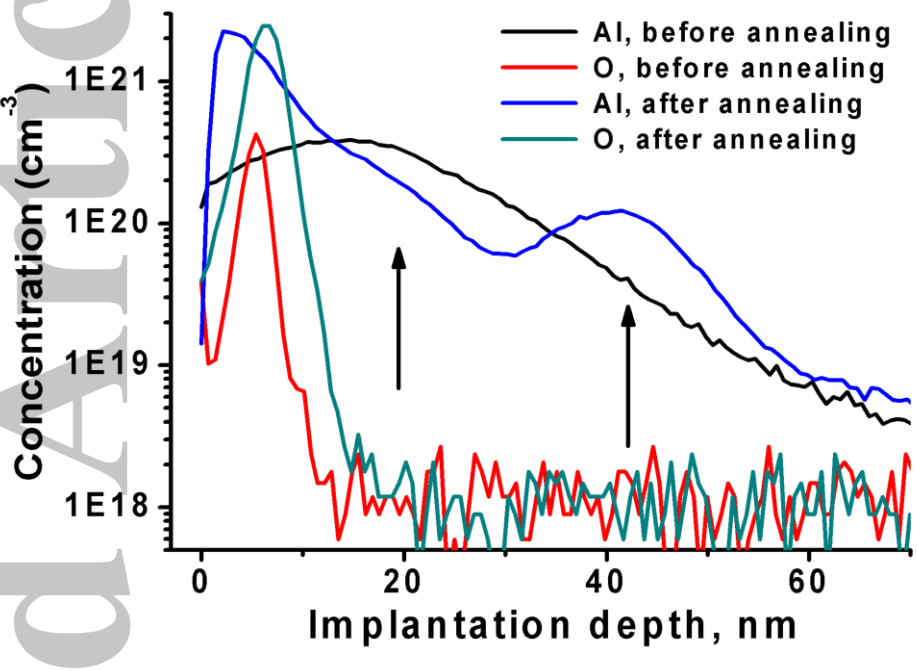

Fig. 4. ToF-SIMS depth profiles of aluminum and oxygen in Si samples before and after annealing at 800 ℃ for 30 min. The projectiles are Al_2 clusters with energy of 20 keV. The arrows show peaks corresponding to aluminum precipitates